Scripta Materialia 116 (2016) 135–138

Contents lists available at ScienceDirect

Scripta Materialia

journal homepage: www.elsevier.com/locate/scriptamat

Regular Article

Microstructure and lap shear strength of the weld interface in ultrasonic welding of Al alloy to stainless steel

Hiromichi T. Fujii *, Yuta Goto, Yutaka S. Sato, Hiroyuki Kokawa

Department of Materials Processing, Graduate School of Engineering, Tohoku University, 6-6-02 Aramaki-aza-Aoba, Aoba-ku, Sendai 980-8579, Japan

ARTICLE INFO

Article history:
Received 23 October 2015
Received in revised form 2 February 2016
Accepted 3 February 2016
Available online xxxx

Keywords:
Ultrasonic welding
Al alloy 6061
304 stainless steel
Shear deformation
Recrystallization

ABSTRACT

Dissimilar welds between Al alloy and stainless steel were produced with an ultrasonic welding technique. The weld strength increased with the welding energy. The welds produced with sufficiently high energy exhibited nugget pull-out failure of the Al alloy during the lap shear strength test. The welds with weld energies of more than 1.05 kJ fractured in the base metal and were severely deformed by the ultrasonic vibration, and recrystallization occurred around the weld interface owing to the shear deformation and heating during the ultrasonic welding.

Global environmental issues have led to a demand for increasing the mass efficiency of industrial products. One suggested solution has been the development of welding technology for multi-material design. Parts of conventional steel components are replaced with lighter materials through various dissimilar welding techniques to reduce the vehicle weight and improve fuel efficiency. The ultrasonic welding (USW) technique has been the subject of several studies because it can be used to achieve dissimilar welds between Al alloy and steel sheets with limited interface intermetallic reaction [1–3]. USW is a solid-state welding technique that is characterized by a lower energy input, a shorter welding time, and thinner workpieces than other welding techniques.

There have been several studies on USW to clarify the weld properties since it was first used to successfully weld metallic sheets together in the 1950s [4–8]. Many metallurgical phenomena around the weld interface have been found to significantly contribute to the mechanical behavior of the weld. Gunduz et al. welded 1100 H19 Al foil to a pure Zn sheet and revealed that the diffusivity of Zn in Al significantly increases around the weld interface during USW [9]. The estimated value of diffusivity was 1.9 $\mu m^2/s$, which is approximately 10^5 times higher than the normal lattice diffusivity. Additionally, they found that the phase stability changes around the weld interface owing to deformation-induced vacancies. Bakavos et al. used ultrasonic spot welding on 6111 Al automotive sheets and observed the material flow characterized by swirls of grains [10]. Many researchers have used the lap shear strength to characterize the mechanical properties of an ultrasonic weld [2,10–15]. In the tensile test, the fracture mode was found to change from interfacial debonding to nugget pull-out above a threshold welding energy.

Although many studies have been conducted on USW [16–36] in addition to the ones described above, knowledge on the dependence of the microstructure on the mechanical properties of the ultrasonic weld is limited. Moreover, there is currently little academic understanding on the welding mechanism of Al–steel USW despite its engineering significance and past research efforts [1–3,31]. The aim of the current work was to clarify the lap shear strength of the ultrasonic welds between Al alloy and stainless steel and the microstructural characteristics around the weld interface. The results can substantially contribute to the understanding of welding mechanisms involved in achieving sound ultrasonic welds between dissimilar metals.

This study used sheets of the commercial Al alloy 6061-T6 and 304 stainless steel sheets with dimensions of $50 \times 20 \times 1.0$ mm^3 and $50 \times 20 \times 0.5$ mm^3, respectively. The rolling direction (RD) of the specimens was set perpendicular to the direction of ultrasonic vibration. The shape of the horn tip was a square with 6 mm sides; thus, the welding area was approximately 6×6 mm^2. The surfaces of the ultrasonic horn and anvil were knurled to prevent them from slipping on the specimen surfaces. Table 1 lists the welding parameters used in this study. The welding energy of the table was estimated from the time integral of the welding machine power during USW. It exhibited a proportional relationship to the welding time. During USW, the temperature was measured by using a type-K thermocouple embedded on the interface between the Al alloy 6061-T6 and 304 stainless steel sheets.

To evaluate the weld strength of the specimens, a lap shear tensile strength test was employed at a crosshead speed of 3 mm/min. The tensile direction was set perpendicular to the direction of ultrasonic

* Corresponding author.

http://dx.doi.org/10.1016/j.scriptamat.2016.02.004
1359-6462/

Table 1
Ultrasonic welding conditions in this study.

Material	Thickness, *t* (mm)	Ultrasonic vibration		Normal load, *F* (N)	Clamping pressure, *C* (MPa)	Welding energy, *E* (kJ)	Welding power, *P* (kW)
		Frequency, *f* (kHz)	Amplitude, *A* (μm)				
6061 Al alloy 304 stainless steel	1.0 0.5	19.15	51	589	0.3	0.20–1.20	0.90–1.06

vibration. The microstructures of the welds were characterized with a field emission gun scanning electron microscope (FEG-SEM) equipped with an electron backscattered diffraction (EBSD) system. The electron beam was scanned at step sizes of 0.7 μm on the transverse direction–normal direction (TD–ND) plane. Grain boundaries with a misorientation angle of less than 15° were defined as low-angle grain boundaries (LABs), and those with an angle of more than 15° were defined as high-angle grain boundaries (HABs).

Fig. 1(a) shows the dependence of the lap shear strength on the welding energy of the welded specimens. The specimens were not welded when the welding energy was less than 0.4 kJ. The lap shear strength increased with the welding energy before plateauing at 2.0–2.8 kN. Fig. 1(b) shows examples of the typical fracture surfaces of tensile-tested coupons for five different welding energy inputs. The welded area increased with the welding energy up to 0.9 kJ and then reached the contact area between the ultrasonic horn and Al alloy during welding. The fracture mode changed from interface debonding to nugget pull-out when the energy input was more than 1.0 kJ. To determine the reason for this change in fracture mode, the microstructure around the weld interface and the welding mechanism were characterized.

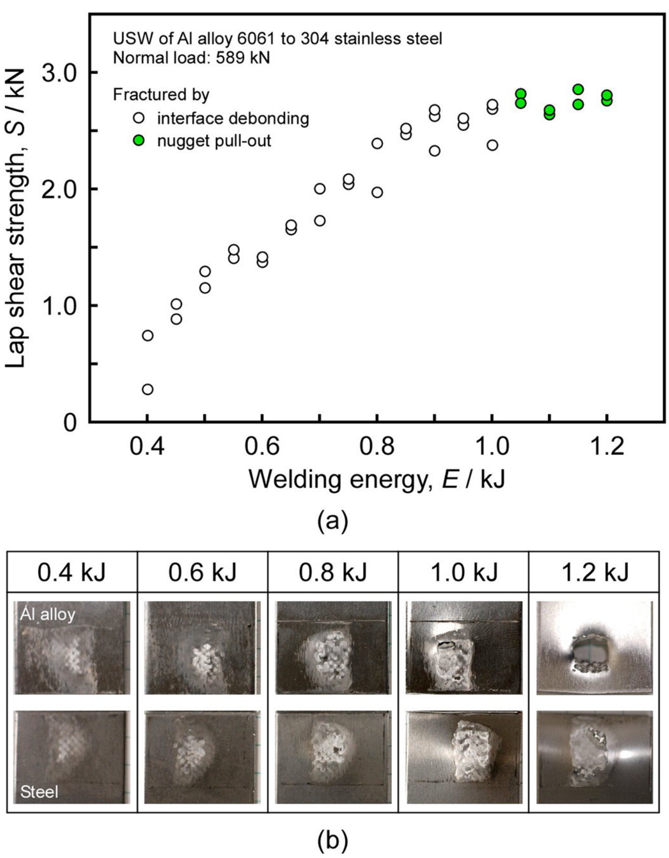

Fig. 1. (a) Relationship between the lap shear strength and welding energy in ultrasonic welding of 6061 Al alloy to 304 stainless steel and (b) the fractured specimens in the lap shear strength test.

In order to examine the detailed grain structure and texture, an EBSD analysis was performed around the weld interface. Fig. 2(a) and (b) give the grain boundary characteristic distribution maps of the specimens welded at energies of 0.65 and 1.15 kJ, respectively. Although the grains structure of Al alloy region had roughly the same microstructure as the base material in the specimen welded at a 0.65 kJ energy input, the deformed microstructure was locally found at the weld interface. In contrast, all Al grains close to the weld interface were fine and equiaxed in the specimen welded at 1.15 kJ. Based on the microstructural characteristics, the microstructure of Al alloy was divided into two regions, as shown in Fig. 2(b). The area consisting of fine and equiaxed grains was defined as the interface region, and the rest was defined as the bulk region. Table 2 summarizes the fractions of LABs and HABs obtained from each region in Fig. 2(a). The fraction of LABs significantly increased in the bulk and interface regions of the specimen welded at the energy input of 1.15 kJ. The data imply that the severe plastic deformation associated with ultrasonic vibration increased the welded area, which increased the weld strength. In addition, the fraction of LABs in the interface region was smaller than that in bulk region in the specimen welded at the energy input of 1.15 kJ. This resulted from recrystallization due to shear deformation and deformation heating during USW. Consequently, fine and equiaxed grains were formed around the weld interface.

To understand the deformation behavior during USW, texture analyses were applied to each region as shown in Fig. 2(a) and (b). Fig. 2(c)–(e) show {111} pole figures extracted from (c) the bulk region of Al alloy in the specimens welded at 0.65 kJ (Fig. 2(a)) and (d) the interface and (e) bulk regions of the Al alloy in the specimens welded at 1.15 kJ (Fig. 2(b)). No significant changes in texture were observed in the bulk regions of the specimens. In contrast, a {111}<110> component, which is one of the ideal simple shear orientations [37], was developed in the interface region of the specimen welded at 1.15 kJ as shown in Fig. 2(e). This consistent result indicates that the {111} slip planes and <110> slip directions of the grains lie on the welding plane in the interface region. This would be attributed to the shear deformation of micro-asperities on the Al alloy surface, which was caused by the friction between Al alloy and stainless steel sheets with ultrasonic vibration. Thus, severe shear deformation parallel to the welding interface can be concluded to significantly contribute to the weld performance and microstructural evolution around the weld interface during USW.

Thermal measurements were performed to further verify the above microstructural evolution during USW. Fig. 3 presents the thermal profiles for the interface between the Al alloy and stainless steel sheets during USW. The heating time during USW was approximately 1–2 s. The peak temperature increased with the welding energy from approximately 450 K to 600 K. In general, a temperature of 600 K and heating time of 2 s are not sufficient to form recrystallized grains in 6061 Al alloy [38]. However, the interface region was found to contain a high number of dislocations owing to the severe plastic deformation. According to Gunduz et al. [9], the vacancy concentration and diffusivity of atoms are significantly increased by the high-strain-rate deformation around the weld interface region during USW. These facts suggest that recrystallization occurs around the weld interface even at low temperatures and short heating times during USW. Therefore, the interfacial microstructure of the ultrasonic weld between the Al alloy and stainless steel would develop with the progression of recrystallization.